

## 摘要

由于 PEG 修饰能够有效延长递送体系的血液循环时间, PEG 修饰的脂质体药物递送体系在癌症治疗中具有广泛的应用。然而, PEG 修饰会阻碍体系的细胞内吞, 其严重影响药物递送体系在肿瘤部位的富集和疗效。更为重要的是, PEG 修饰的脂质体负载细胞周期性药物拓扑替康时会引发加快血液清除 (ABC) 现象, 这一现象严重降低了药物递送脂质体在肿瘤部位的富集, 给脂质体药物递送体系带来严重挑战。为了解决这一问题, 我们构建了两性离子聚合物聚羧基三甲胺乙内酯 PCB 修饰的脂质体药物递送体系。PCB 同 PEG 一样能够抵抗蛋白吸附而增强脂质体的血清稳定性。不同的是, pH 敏感的 PCB 修饰脂质体能够通过细胞内吞方式高效进入细胞, 实现药物可控释放。同时, PCB 脂质体能够避免 ABC 现象, 促进药物递送体系在肿瘤部位的富集, 从而有效提高体系的肿瘤抑制效果, 为肿瘤治疗提供了新的策略。



# Enhanced retention and anti-tumor efficacy of liposomes by changing their cellular uptake and pharmacokinetics behavior



Yan Li <sup>a, b, 1</sup>, Ruiyuan Liu <sup>a, c, 1</sup>, Jun Yang <sup>a</sup>, Yuanjie Shi <sup>d</sup>, Guanghui Ma <sup>a</sup>,  
Zhenzhong Zhang <sup>c, \*\*</sup>, Xin Zhang <sup>a, \*</sup>

<sup>a</sup> National Key Laboratory of Biochemical Engineering, Institute of Process Engineering, Chinese Academy of Sciences, Beijing 100190, PR China

<sup>b</sup> University of Chinese Academy of Sciences, Beijing 100049, PR China

<sup>c</sup> School of Pharmaceutical Sciences, Zhengzhou University, 100 Kexue Avenue, Zhengzhou 450001, PR China

<sup>d</sup> School of Life Sciences, University of Beijing Institute of Technology, Beijing 100081, PR China

## ARTICLE INFO

### Article history:

Received 25 July 2014

Accepted 7 November 2014

Available online

### Keywords:

Liposomes

Poly(carboxybetaine)

Poly(ethylene glycol)

Accelerated blood clearance phenomenon

Tumor accumulation

## ABSTRACT

Although PEGylated liposome-based drug delivery systems hold great promising applications for cancer therapy due to their prolonged blood circulation time, PEGylation significantly reduces their cellular uptake, which markedly impairs the *in vivo* tumor retention and antitumor efficiency of drug-loaded liposomes. Most importantly, it has been proved that repeated injections of PEGylated liposomes with cell cycle specific drug such as topotecan (TPT) in the same animal at certain time intervals will induce “accelerated blood clearance” (ABC) phenomenon, which decreases the tumor accumulation of drug-loaded liposomes and presents a tremendous challenge to the clinical use of liposome-based drug delivery systems. Herein, we developed a zwitterionic poly(carboxybetaine) (PCB) modified liposome-based drug delivery system. The presence of PCB could avoid protein adsorption and enhance the stability of liposomes as that for PEG. Quite different from the PEGylated liposomes, the pH-sensitive PCBylated liposomes were internalized into cells *via* endocytosis with excellent cellular uptake and drug release ability. Furthermore, the PCBylated liposomes would avoid ABC phenomenon, which promoted the tumor accumulation of drug-loaded liposomes *in vivo*. With higher tumor accumulation and cellular uptake, the PCBylated drug-loaded liposomes significantly inhibited tumor growth and provided a promising approach for cancer therapy.

© 2014 Elsevier Ltd. All rights reserved.

## 1. Introduction

Widely recognized for their ability to produce a prolonged blood circulation time and facilitate tumor accumulation *via* the enhanced permeability and retention (EPR) effect, PEGylated liposome-based drug delivery systems hold great promising applications for cancer therapy [1–4]. Unfortunately, PEGylation significantly reduces the cellular uptake and endosomal/lysosomal escape of the liposomes, and interferes with the tumor retention and antitumor efficacy of liposome-based drug delivery systems [5,6]. Most importantly, it has been proved that repeated injections of PEGylated liposomes with cell cycle specific drugs such as

topotecan (TPT) in the same animal at certain time intervals will induce “accelerated blood clearance” (ABC) phenomenon [7,8]. PEGylated drug-loaded liposomes are intended to stimulate the spleen to produce anti-PEG IgM after the first administration, which selectively binds to PEG on the surface of the second administrated liposomes to cause rapid elimination and enhanced hepatic uptake [9,10]. This immune response decreases the tumor accumulation of drug-loaded liposomes and presents a tremendous challenge to the clinical use of liposome-based drug delivery systems.

Advancement in nanotechnology has allowed for the development of delivery systems to avoid the induction of ABC phenomenon through changing the physicochemical properties of the PEGylated liposome-based drug delivery systems [11]. Unfortunately, most of these approaches were accompanied with sacrificing the therapeutic efficacy of PEGylated liposomes. It has been shown that liposomes modified with cleavable PEG-lipid derivatives could avoid the induction of ABC phenomenon.

\* Corresponding author. Fax: +86 010 82544853.

\*\* Corresponding author. Fax: +86 371 67781908.

E-mail addresses: [zhangzz08@126.com](mailto:zhangzz08@126.com) (Z. Zhang), [xzhang@ipe.ac.cn](mailto:xzhang@ipe.ac.cn) (X. Zhang).

<sup>1</sup> These authors contributed equally to this work.

However, the effect on long circulation of the cleavable PEGylated liposomes was worse than that of non-cleavable PEGylated liposomes [12].

Another approach has focused on the use of alternative polymers to extend the circulation time of liposome-based drug delivery systems [13]. In our previous study, it has been proved that zwitterionic polymer poly(carboxybetaine) (PCB) has superior ability in extending the blood retention without interfering with the cellular uptake and endosomal/lysosomal escape of the liposomes, which is quite different from that of PEGylation [14]. However, whether liposome-based drug delivery systems modified with PCB would avoid ABC phenomenon *in vivo* has not been verified. Herein, to address the challenge, the performances of PCBylated liposome-based drug delivery systems in cellular uptake, pharmacokinetics and tumor therapy were investigated. Our findings demonstrated that PCBylation could change the cellular uptake behavior and avoid ABC phenomenon of drug-loaded liposomes, which facilitated the tumor accumulation and therefore enhanced the antitumor activity of liposome-based drug delivery systems (Scheme 1).

## 2. Materials and methods

### 2.1. Materials

1,2-Distearoyl-*sn*-glycero-3-phosphoethanolamine-*n*-[methoxy (polyethylene glycol)-2000] (DSPE-PEG 2000), 1-palmitoyl-2-oleoyl-*sn*-glycero-3-phosphocholine (POPC), cholesterol were purchased from Advanced Vehicle Technology Ltd., Co. (Shanghai, China). Doxorubicin (DOX) and topotecan hydrochloride (TPT) were obtained from Melonepharma (Dalian, China). (5-Dimethylthiazol-2-yl)-2, 5-diphenyltetrazolium bromide (MTT), FITC-phalloidin and 4',6-diamidino-2-phenylindole dihydrochloride (DAPI) were obtained from Sigma–Aldrich. Lyso-Tracker Green and Annexin V-FITC apoptosis detection kit were obtained from Invitrogen. Dulbecco's Modified Eagle Medium (DMEM), penicillin (10,000 U/mL), streptomycin (10 mg/mL), trypsin-EDTA and fetal bovine serum (FBS) were purchased from Thermo. All other reagents used were obtained commercially at analytical grade.

Male SD rats weighting 200–250 g and male BALB/c nu/nu mice weighting 20–25 g were purchased from the Academy of Military Medical Sciences of China. The animal had free access to water and animal chow. All procedures involving experimental animals were carried out in accordance with the protocols approved by the Institutional Animals Care and Use Committee of Peking University.

### 2.2. Preparation and characterization of empty and drug-loaded liposomes

The empty liposomes modified with distearoyl phosphoethanolamine-poly(carboxybetaine)<sub>20</sub> (DSPE-PCB<sub>20</sub>) were prepared by thin lipid film method. Briefly, the mixture of POPC, cholesterol and DSPE-PCB<sub>20</sub> (50: 40: 10, molar ratio) were dissolved in 20 mL of chloroform and dried to a thin lipid film under a stream of N<sub>2</sub> gas, followed by incubation overnight under vacuum to remove residual solvent. The dried lipid films were subsequently hydrated in 10 mL of 200 mM ammonium sulfate. After sonication at 37 °C for 30 min, the solution was extruded 5 times using EmulsiFlex-C5 high-pressure homogenizer (Avestin, Canada).

The liposomes with drugs of DOX or TPT were prepared using the method of ammonium sulfate gradient. The external buffer of the liposomes was exchanged by dialyzing the empty liposomes against PBS (pH = 7.4) for 3 h. Subsequently, the liposomes and DOX or TPT solution (10:2, weight ratio) were incubated for 30 min at 60 °C. Non-entrapped free DOX or TPT was removed by dialyzing the liposomes against PBS (pH = 7.4) for 24 h at room temperature. The DSPE-PEG 2000 liposomes with the same drugs were prepared by the same way.

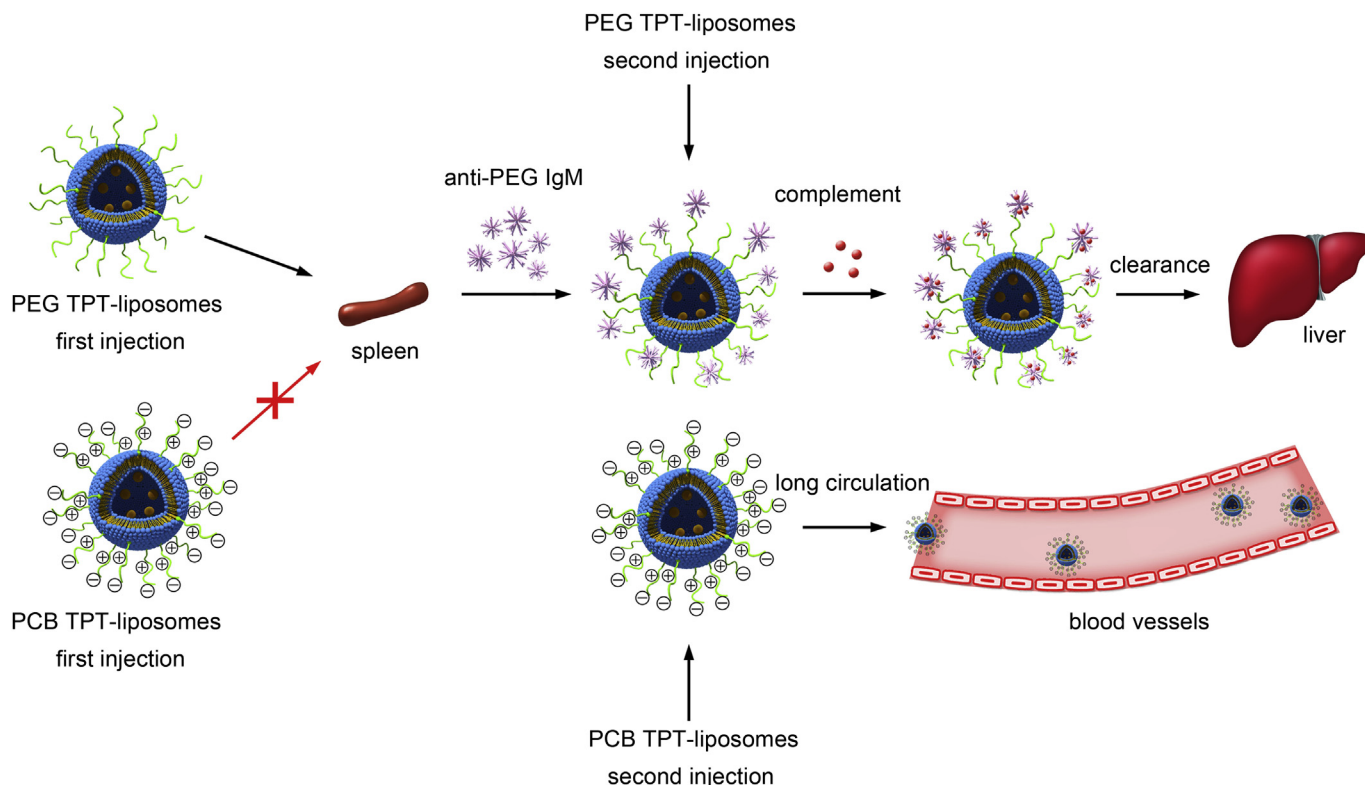
The mean particle diameters of the empty and drug-loaded liposomes were detected by dynamic light scattering (DLS), and the surface charge was analyzed by the zeta potential using a Zetasizer Nano ZS instrument (Malvern Instruments). Further morphological analysis was carried out by cryogenic transmission electron microscopy (Cryo-TEM, FEI Tecnai 20, Netherlands).

### 2.3. Encapsulation efficiency (EE) and drug loading content of liposomes

The encapsulation efficiency and drug loading content of DOX or TPT in liposomal samples were assessed by its UV absorption at the wavelength of 485 nm (DOX) or 360 nm (TPT) on a UV spectrophotometer (TU-1810, Beijing, China). The calibration curves were generated using known concentration of DOX or TPT. The drug loading content and encapsulation efficiency were calculated using the formula:

$$\text{Encapsulation efficiency (\%)} = W_2/W_1 \times 100\%$$

$$\text{Drug loading content (\%)} = W_2/W_0 \times 100\%$$



**Scheme 1.** Schematic illustration of the ABC process of the PCBylated and PEGylated drug-loaded liposomes.

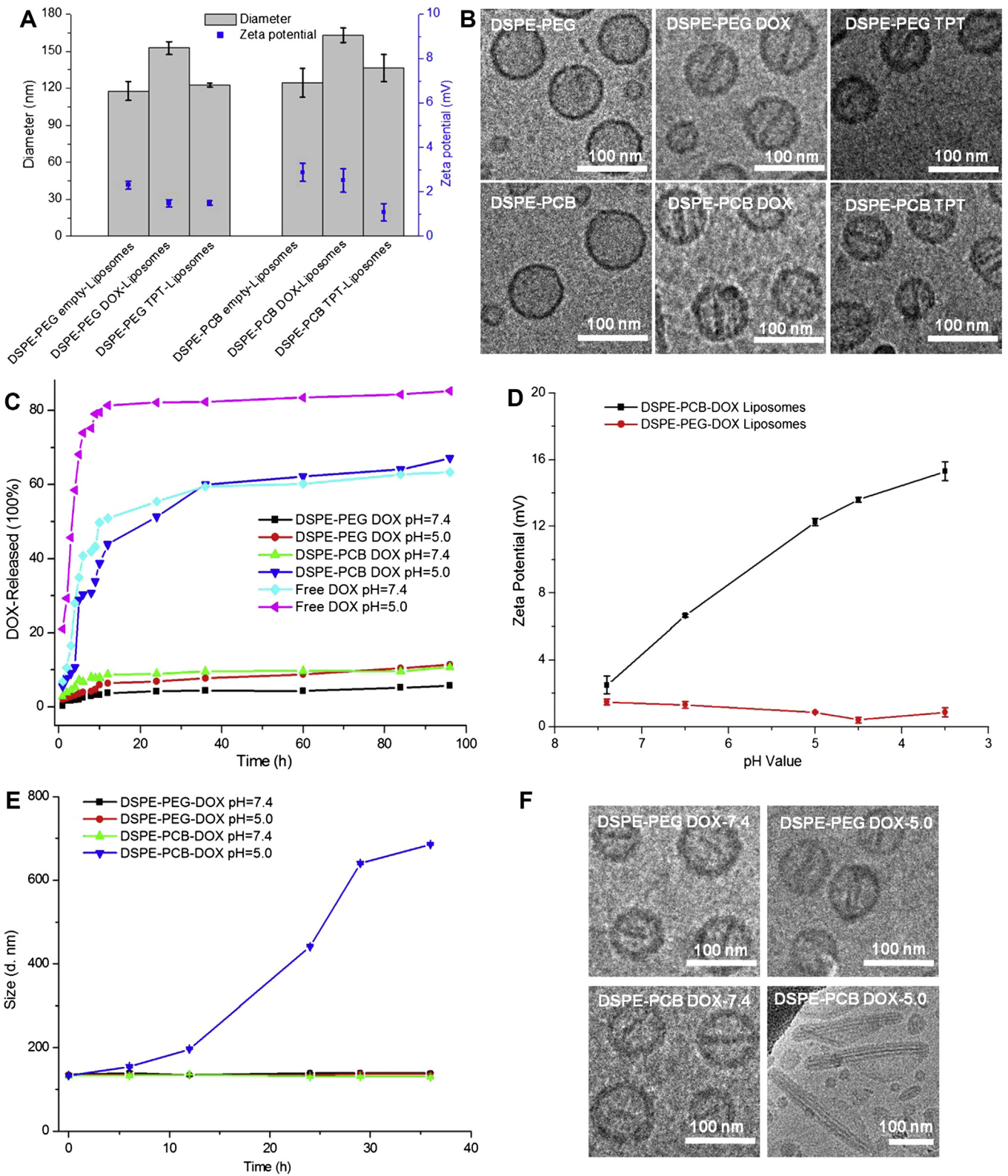


**Fig. 1.** Characterization of empty and drug-loaded liposomes. A) Diameter and zeta potential of the empty and drug-loaded liposomes. B) Cryo-TEM images of the empty and drug-loaded liposomes (scale bar 100 nm). C) Drug release profiles for free DOX, PEGylated and PCBylated DOX-loaded liposomes at pH 7.4 and 5.0 after 96 h incubation, respectively. D) Changes in zeta potential of the PEGylated and PCBylated DOX-liposomes as a function of different pH values. E) Changes in particle sizes of the PEGylated and PCBylated DOX-liposomes at pH 7.4 and 5.0. F) Cryo-TEM images of the DOX-loaded liposomes at pH 7.4 and 5.0 after 12 h incubation (scale bar 100 nm). Data are shown as the mean  $\pm$  S.D. of three independent experiments.

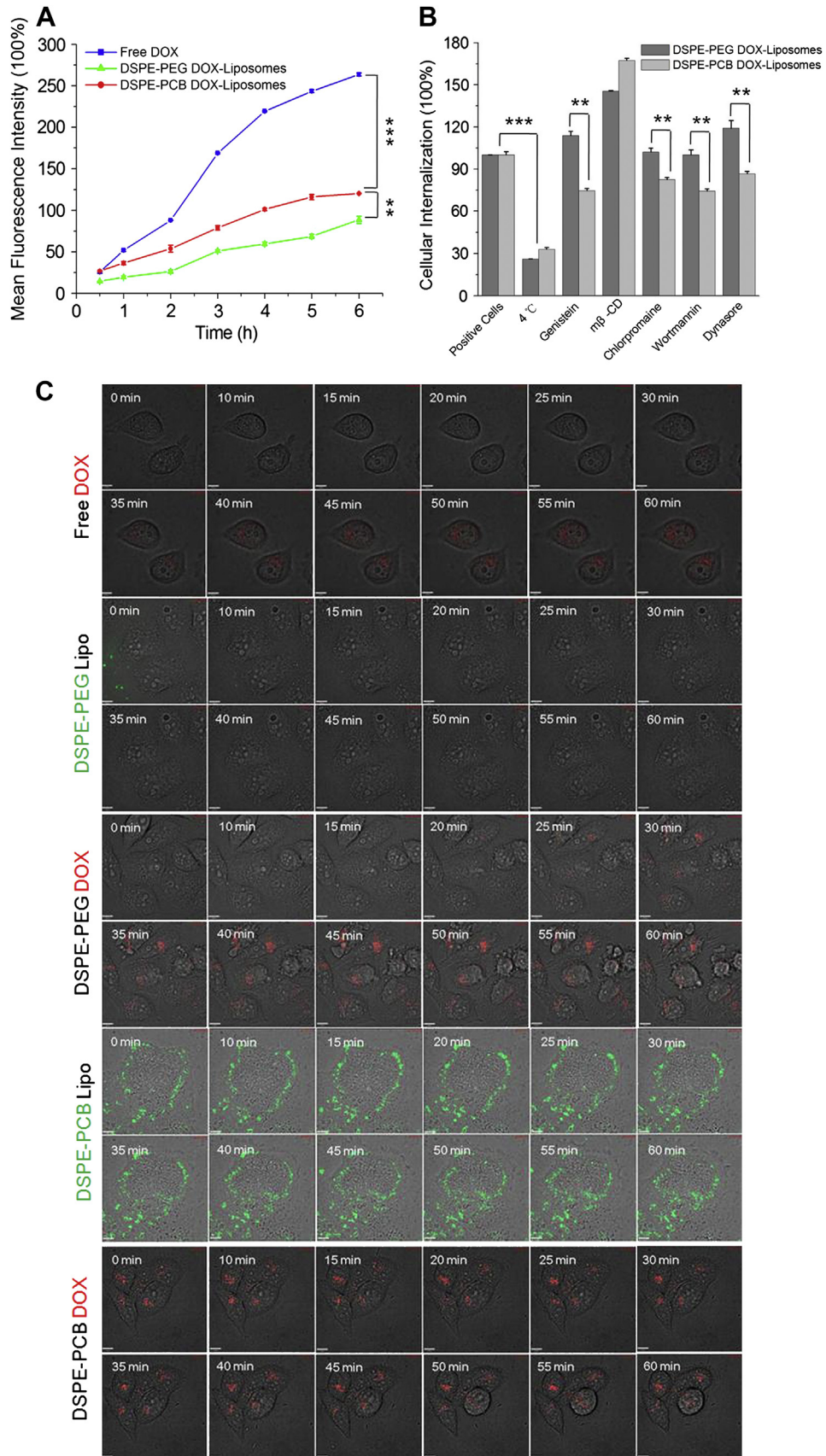


**Fig. 2.** A) Cellular uptake of free DOX, DSPE-PEG and DSPE-PCB DOX-liposomes in A549 cells with the extension of time. The fluorescence of DOX was detected by flow cytometry. B) Mechanistic probes of the intracellular kinetics of DSPE-PEG and DSPE-PCB DOX-liposomes in A549 cells by monitoring the cellular uptake level at 4 °C or in the presence of various endocytic inhibitors. C) Spinning disk confocal image in real-time of A549 cells following incubation with free DOX, DOX-liposomes and rhodamine B labeled empty-liposomes at 37 °C for 1 h, respectively.

where  $W_2$  was the weight of DOX or TPT in liposomes,  $W_1$  was the weight of DOX or TPT used for encapsulating and  $W_0$  was the weight of total liposomes.

#### 2.4. Stability of liposomes

To determine the serum stability of the liposome-based drug delivery systems, liposomes with drugs at a concentration of 1 mg/mL were incubated in DMEM containing 10% FBS at 37 °C. At each time point, the mean diameters of the liposomes were calculated in triplicate using DLS.

To assess the physically stability of the liposome-based drug delivery systems, liposomes encapsulating drugs were placed at 4 °C. At designed time point, the mean diameters of the liposomes were detected in triplicate using DLS.

#### 2.5. Zeta potential measurements of liposomes at different pH

The liposomes with drugs were incubated in phosphate buffer (PB) solution of different pH at 37 °C for 30 min. The zeta potential of the liposomes was measured with a Zetasizer Nano ZS instrument (Malvern Instruments, USA).

#### 2.6. Drug release ability of liposomes

The dialysis method was applied to monitor the *in vitro* release of drugs from drug-loaded liposomes at pH 7.4 and 5.0, respectively. Briefly, drug-loaded liposomes were suspended in 3.0 mL PBS (pH = 7.4) in a dialysis bag (MWCO 3500) and were incubated in 50 mL PBS or PB with pH of 5.0 at 37 °C under horizontal shaking (150 rpm). At predetermined time intervals, the aliquots of incubation medium were removed and the same volume of fresh solution was added. The concentration of drug in the incubation medium was detected using high performance liquid chromatography (HPLC) assay, which equipped with a UV detector and a Phenomenex C<sub>18</sub> column at 25 °C (Shimadzu, Japan).

The HPLC condition for DOX was as follows: the mobile phase was ethanol, acetonitrile, 0.01 mol/L ammonium dihydrogen phosphate and glacial acetic acid (50: 20: 28: 0.6, volume ratio, HPLC grade) at a flow rate of 1.0 mL/min. A wavelength of 480 nm was used to detect the concentration of DOX. Concentration of free DOX was determined based on the peak area at the retention time of 4.9 min according to the calibration curve.

The HPLC condition for TPT was as follows: the mobile phase was double distilled water, acetonitrile and trifluoroacetic acid (80: 20: 0.1, volume ratio, HPLC grade) at a flow rate of 0.8 mL/min. A wavelength of 360 nm was used to detect the concentration of TPT. Concentration of TPT was determined based on the peak area at the retention time of 10 min according to the calibration curve.

The release percentage of drugs was calculated using the formula:

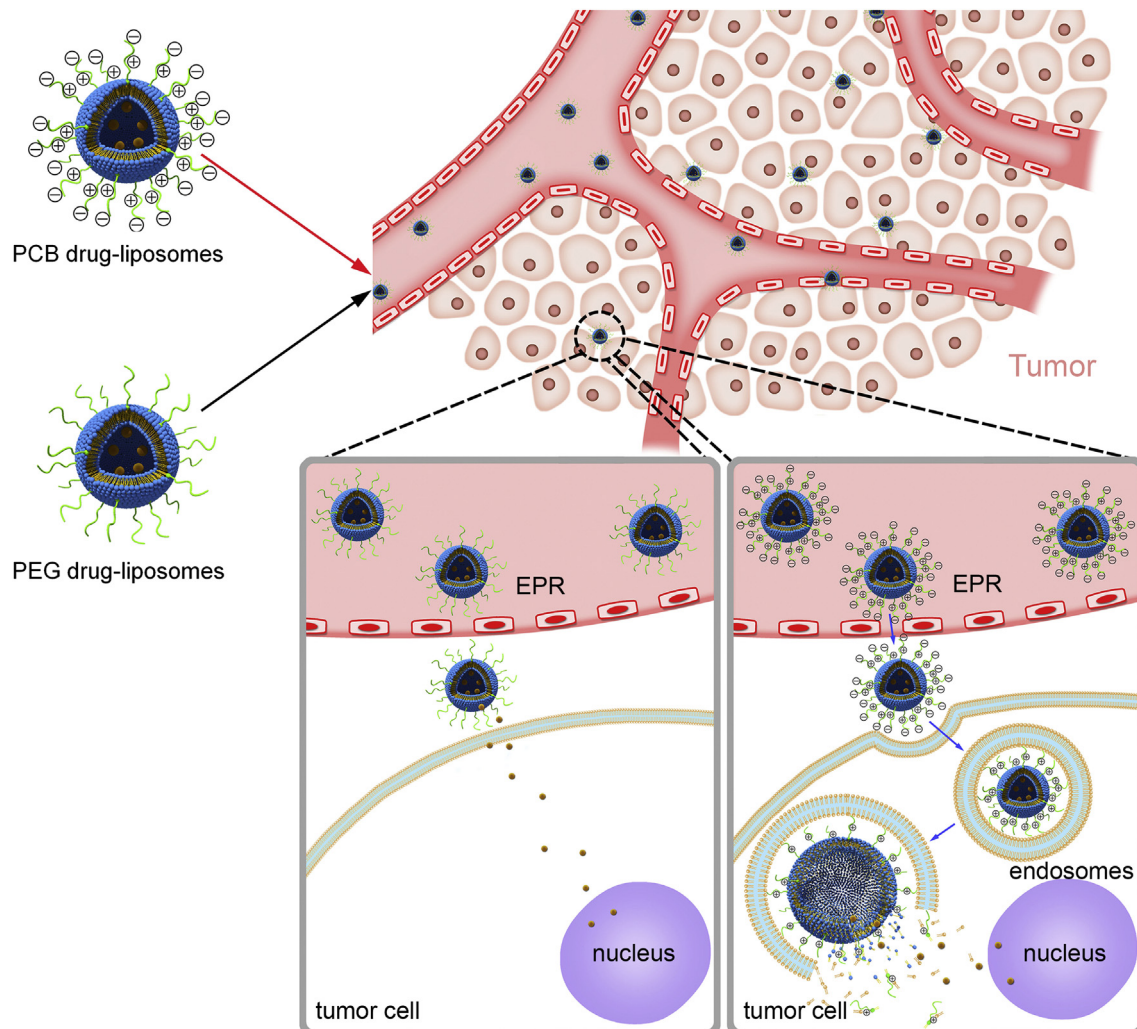
$$\text{Release percentage (\%)} = W_1/W_0 \times 100\%$$

where  $W_1$  was the weight of drugs in solution,  $W_0$  was the weight of total drugs in liposomes.

#### 2.7. Cellular uptake of liposomes detected by flow cytometry measurements

For flow cytometric analysis, A549 cells were seeded into 12-well plates at  $2 \times 10^5$  cells per well with 0.5 mL of complete DMEM culture medium for 24 h. The medium was replaced with 0.5 mL of DMEM medium with 10% FBS containing DOX-liposomes. The concentration of DOX was 5 µg/mL. The cells were further incubated for specific periods of time, and then washed three times with cold PBS, trypsinized and harvested in PBS. The samples were then assessed with BD Calibur flow cytometry (BD Co., USA) to determine the fluorescence intensity of DOX.

To elucidate the endocytic mechanism that was responsible for internalization of PCB or PEG modified liposome-based drug delivery systems, the cellular uptake studies were performed at 4 °C or in the presence of various endocytic inhibitors for



**Scheme 2.** Schematic diagram of the cellular uptake behavior of the DSPE-PCB and DSPE-PEG drug-loaded liposomes.

2 h. Briefly, A549 cells were preincubated with endocytic inhibitors including genistein (100  $\mu\text{g}/\text{mL}$ ), methyl- $\beta$ -cyclodextrin (m $\beta$ CD, 5 mM), chlorpromazine (10  $\mu\text{g}/\text{mL}$ ), dynasore (10  $\mu\text{g}/\text{mL}$ ) and wortmannin (50  $\mu\text{g}/\text{mL}$ ) for 30 min prior to the addition liposomes. The cells were then incubated with DOX-liposomes for 2 h at 37  $^{\circ}\text{C}$ . Results were expressed as the uptake percentage of control cells that were only incubated with DOX-liposomes at 37  $^{\circ}\text{C}$  for 2 h.

## 2.8. Confocal laser scanning microscopy

The intracellular trafficking of liposomes with DOX was assessed using confocal laser scanning microscopy (CLSM). Briefly,  $4 \times 10^5$  A549 cells were seeded in Petri

dishes for 24 h, and the medium was replaced with DMEM containing 10% FBS, which including DOX-liposomes. The concentration of DOX was 5  $\mu\text{g}/\text{mL}$  and the cells were then incubated for 15 min, 30 min, 45 min, 1 h or 3 h at 37  $^{\circ}\text{C}$ , respectively. Subsequently, the cells were washed three times with PBS followed by staining with LysoTracker Green for 30 min at 37  $^{\circ}\text{C}$ . The cells were washed three times with PBS and fixed with fresh 4% paraformaldehyde for 10 min at room temperature. The cells were then counterstained with DAPI for 10 min to stain the nuclei. Red fluorescence of DOX, blue fluorescence of DAPI and green fluorescence of LysoTracker Green were observed using a Zeiss LSM780 CLSM (Zeiss Co., Germany).

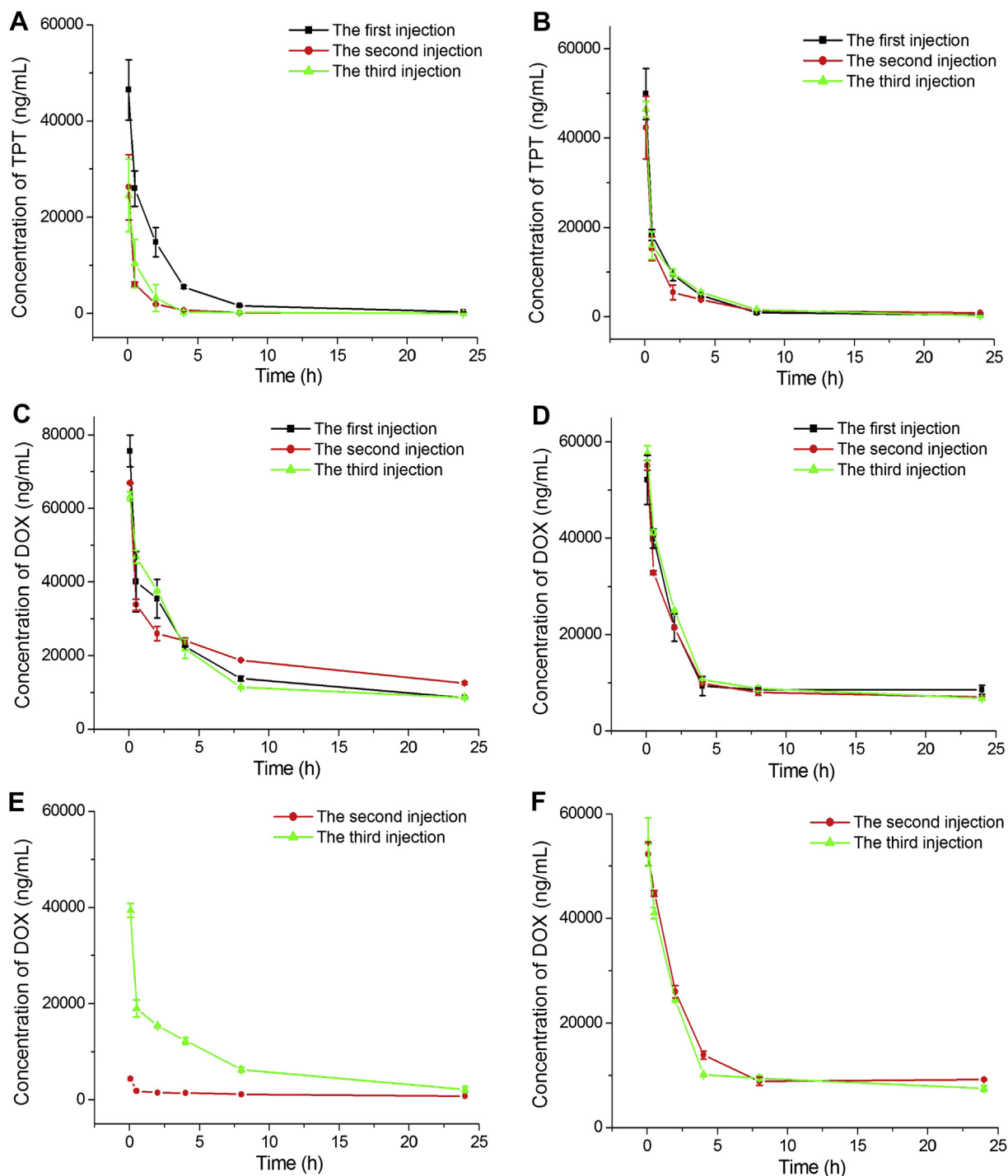


**Fig. 3.** Blood clearance profile of drugs in SD rats. Rats were pretreated with A) DSPE-PEG TPT-liposomes. B) DSPE-PCB TPT-liposomes. C) DSPE-PEG DOX-liposomes. D) DSPE-PCB DOX-liposomes. E) DSPE-PEG empty liposomes as the first injection, and DSPE-PEG DOX-liposomes as the second and third injection. F) DSPE-PCB empty liposomes as the first injection, and DSPE-PCB DOX-liposomes as the second and third injection. The drug concentration was 7 mg/kg and the interval between the two injections was 5 days. \* $P < 0.05$ , \*\* $P < 0.01$ , \*\*\* $P < 0.005$  ( $n = 3$ ).

2.9. Spinning disk confocal image

To observe the cellular uptake of free drug, PCB or PEG modified liposomes in real-time process, cells were detected using spinning disk confocal image. Briefly,  $4 \times 10^5$  A549 cells were seeded in Petri dishes for 24 h, and the medium was replaced with DMEM containing 10% FBS, which including free DOX, DOX-liposomes or rhodamine B labeled empty liposomes. The concentration of DOX was 5  $\mu\text{g}/\text{mL}$ . After 10 min incubation, cells were then observed using UltraVIEW VoX spinning disk confocal image (PerkinElmer, England) for 1 h.

2.10. Cytotoxicity measurement by MTT assay

Drug induced cytotoxicity was determined by the MTT assay. Cells were treated with various concentrations of DOX or TPT for 48 h, respectively. The MTT solution (5 mg/mL) was added to the plates and the plates were then incubated for an additional 3 h. Finally, 100  $\mu\text{L}$  of DMSO was added to each well to dissolve the formazan crystals. The absorbance in each well was determined at 490 nm using a Tecan microplate reader (Tecan, Switzerland). Untreated A549 cells were used as a negative control and its cell viability was defined as 100%.

2.11. Cell apoptosis assay by Annexin V-FITC

For apoptosis analysis,  $5 \times 10^5$  A549 cells per well were cultured in 6-wells plates with 0.5 mL of complete DMEM culture medium for 24 h. The cells were then treated with liposomes with TPT at a concentration of 5  $\mu\text{g}/\text{mL}$ . After 24 h of treatment, apoptosis cells were detected on BD Calibur flow cytometry (BD Co., USA) using the Annexin V-FITC Apoptosis Detection Kit.

2.12. Pharmacokinetics profiles of liposomes in SD rats

SD rats were randomly divided into 7 groups. To determine the pharmacokinetics profiles of liposomes with different modification or different drug, empty liposomes or liposomes with different drugs of DOX or TPT at a dose of 7 mg/kg were administered to SD rats via the tail vein. Control rats received an injection of PBS instead of liposomes. The interval between two injections was 5 days. At the time point of 5 min, 30 min, 2 h, 4 h, 8 h and 24 h following injection, blood samples were collected via eye puncture. Blood samples were centrifuged at  $1180 \times g$  for 10 min to obtain the plasma to determine the pharmacokinetics property of the liposomes.

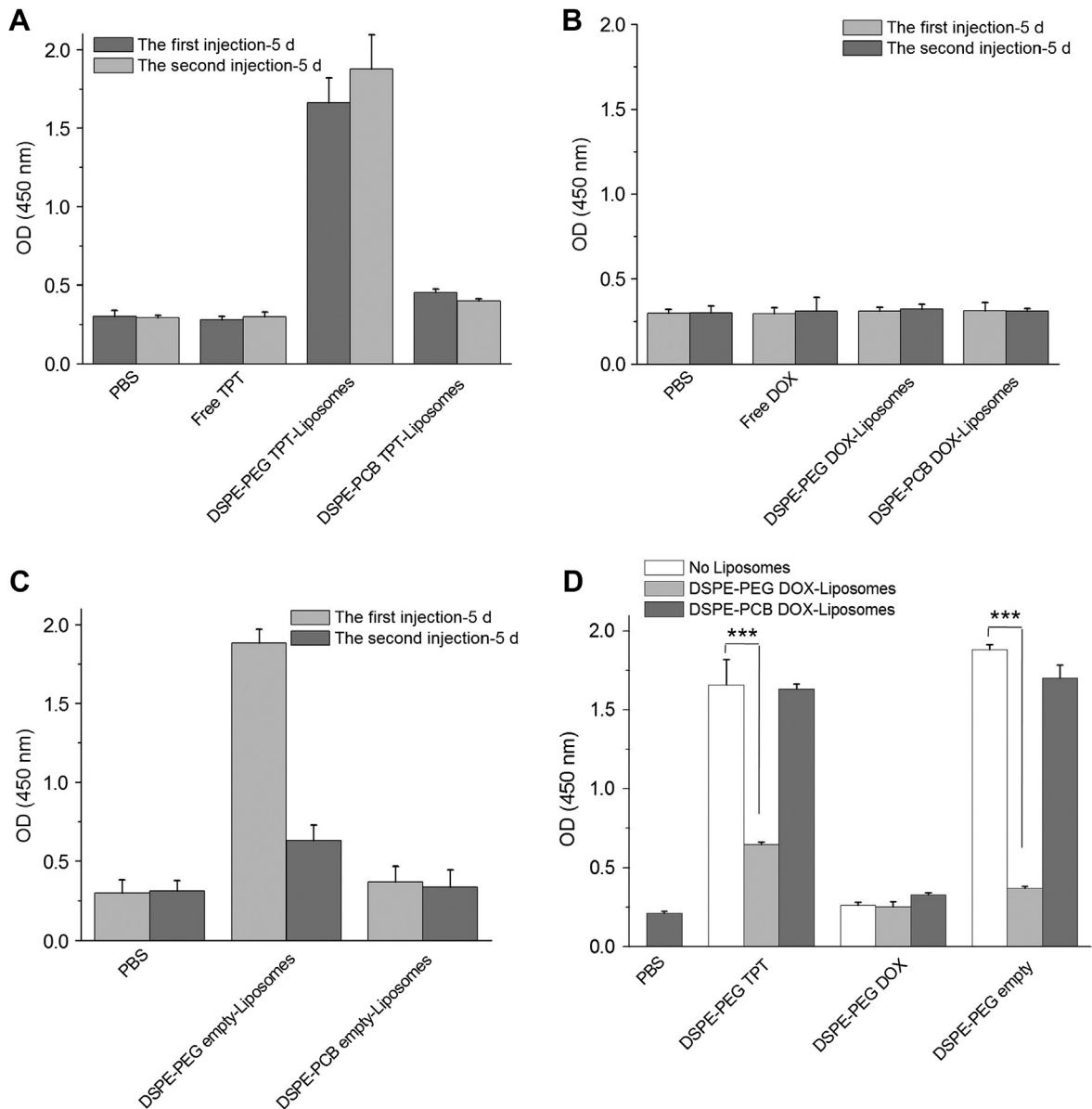


**Fig. 4.** IgM levels in plasma of SD rats following administrated with A) Free TPT, DSPE-PEG and DSPE-PCB TPT-liposomes. B) Free DOX, DSPE-PEG and DSPE-PCB DOX-liposomes. C) DSPE-PEG and DSPE-PCB empty liposomes as the first injection and DOX-liposomes as the second injection. Drug-loaded liposomes were administered to SD rats with drug concentration of 7 mg/kg via the tail vein. The amount of empty liposomes was equal to the drug-loaded liposomes used for injection. The IgM level was detected using ELISA after 5 days of injection. D) IgM levels in plasma after incubation with DSPE-PEG and DSPE-PCB DOX-liposomes at 37 °C for 15 min. The plasma was obtained from SD rats administrated with DSPE-PEG TPT-, DOX- and empty liposomes as mentioned above. \* $P < 0.05$ , \*\* $P < 0.01$ , \*\*\* $P < 0.005$  ( $n = 3$ ).

### 2.13. Quantitative determination of IgM level using ELISA

Plasma samples were collected on day 5 after the first or second dose of DOX-, TPT- or empty liposomes. Plasma samples of rats received PBS were used as a control. The concentration of the IgM was determined using ELISA method according to the manufacturer's instructions. The absorbance was measured at 450 nm using a SpectraMax M5 microplate reader (Molecular Devices, USA).

500  $\mu$ L of plasma samples collected on day 5 after the first injection of DSPE-PEG 2000 modified TPT-, DOX- and empty liposomes were incubated with 125  $\mu$ L of DSPE-PEG 2000 DOX-liposomes or DSPE-PCB DOX-liposomes at 37  $^{\circ}$ C for 15 min. After incubation, liposomes were separated out by centrifugation at  $14,462 \times g$  for 30 min. The IgM in supernatant was detected using ELISA according to the manufacturer's instructions. The absorbance was measured at 450 nm using a SpectraMax M5 microplate reader (Molecular Devices, USA).

### 2.14. Pharmacokinetics profiles and biodistribution study in tumor-bearing mice model

To determine the pharmacokinetics profiles and biodistribution of liposomes with DOX or TPT in A549 tumor-bearing nude mice, liposomes with different drug of DOX or TPT at a dose of 5 mg/kg were administered *via* the tail vein. After 5 days of the first injection, mice were received liposomes with the same drug at a dose of 5 mg/kg. At designed time points following injection, blood samples were collected *via* eye puncture. Blood samples were centrifuged at  $1180 \times g$  for 10 min to obtain the plasma to determine the pharmacokinetics property of the liposomes. After 4 h of each injection, mice were sacrificed and tissues were collected. The drug concentration in each tissue was detected using HPLC using the method above.

The intra-tumor distribution of drug, PCB or PEG modified liposomes in tumor tissue were observed using CLSM. Briefly, tumor-bearing nude mice were received an injection of DOX-loaded or rhodamine B labeled empty liposomes, respectively. After 24 h of each injection, mice were sacrificed and tumor tissues were collected.

Tumor tissues were cross-sectioned using a microtome cryostat followed by staining with FITC-phalloidin for 30 min at room temperature. The cells were washed three times with PBS and then counterstained with DAPI for 10 min to stain the nucleus. The samples were observed using a Zeiss LSM780 CLSM (Zeiss Co., Germany).

### 2.15. Therapeutic efficacy of liposomes in tumor-bearing nude mice model

To evaluate the antitumor efficacy of liposomes with different drug of DOX or TPT, BALB/c nu/nu mice were inoculated subcutaneously with A549 cells. The mice were randomly divided into 7 groups and treated with various formulations *via* the tail vein injection every other day. The doses of DOX or TPT of each injection were fixed at 5 mg/kg. The tumor volume was measured using the formula:

$$V(\text{mm}^3) = (a \times b^2)/2$$

where  $a$  and  $b$  are the major and minor axes of the tumor, respectively.

At last, mice were sacrificed and the main organs (heart, liver, spleen, lung and kidney) and tumor were harvested from the animals. The organs and tumor were fixed in a 4% formaldehyde solution for 24 h at the room temperature. The samples were frozen and sections (10  $\mu$ m in thickness) were cut on a microtome cryostat. Hematoxylin and eosin (H&E) staining was performed following manufacturer's instructions and observed by an IX73 bright field microscopy (Olympus). The cell apoptosis of tumor tissue was also detected by the terminal deoxynucleotide transferase-mediated dUTP nick-end labeling (TUNEL) assay according to the manufacturer's protocol (Vazyme<sup>TM</sup>).

### 2.16. Statistical analysis

Quantitative data were expressed as mean  $\pm$  SD. Means were compared using Student's  $t$  test.  $p$  values  $<0.05$  were considered statistically significant.

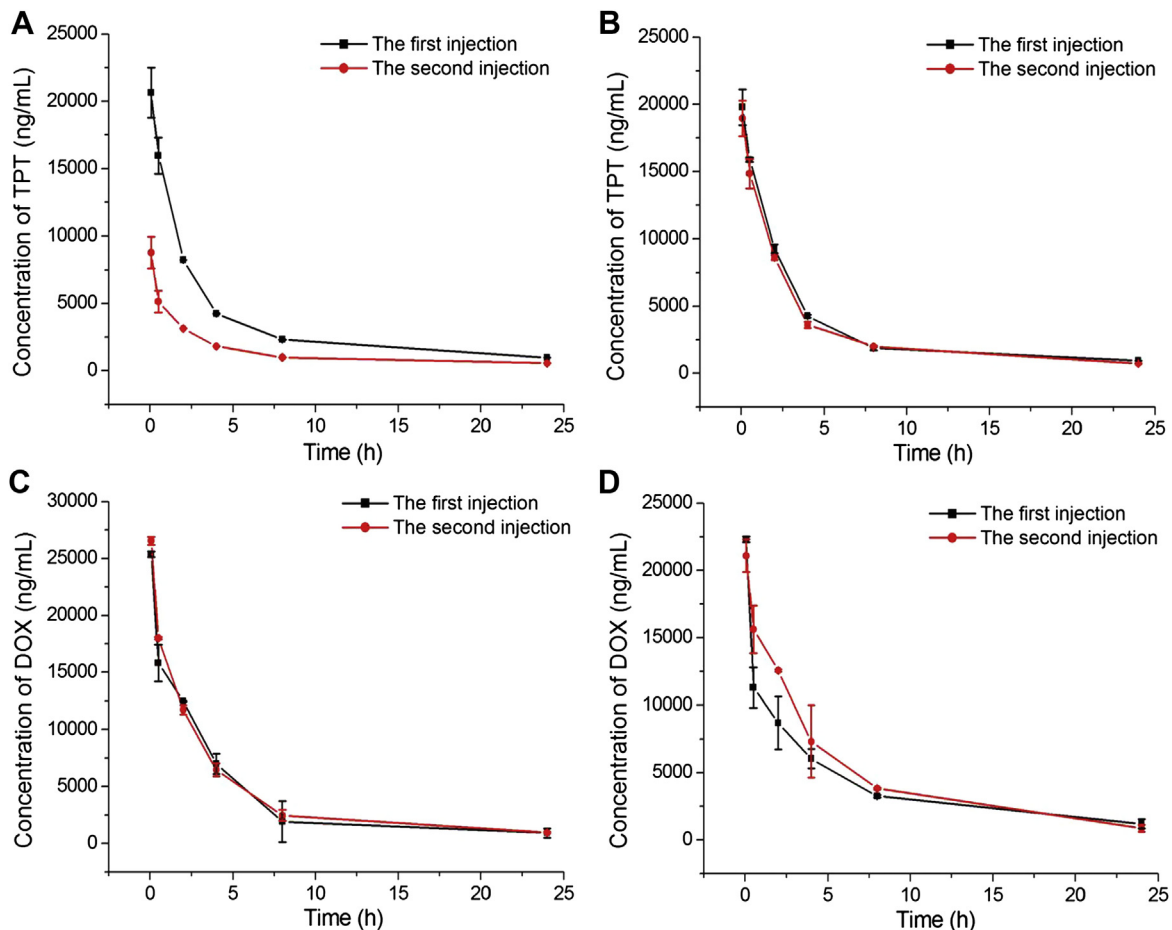


**Fig. 5.** Pharmacokinetic profiles in A549 tumor-bearing nude mice. Mice were pretreated with A) DSPE-PEG TPT-liposomes. B) DSPE-PCB TPT-liposomes. C) DSPE-PEG DOX-liposomes. D) DSPE-PCB DOX-liposomes as the first and second injection. The drug concentration was 5 mg/kg and the interval between the two injections was 5 days. \* $P < 0.05$ , \*\* $P < 0.01$ , \*\*\* $P < 0.005$  ( $n = 3$ ).

### 3. Results and discussion

#### 3.1. Preparation and characterization of empty and drug-loaded liposomes

We first developed PCBylated liposomes with distearoyl phosphoethanolamine-poly(carboxybetaine)<sub>20</sub> (DSPE-PCB<sub>20</sub>), which has been shown comparable ability in prolonging the circulation time of liposomes with that of DSPE-PEG 2000 in our previous work [14]. In order to evaluate the pharmacokinetics and biodistribution of PCBylated liposome-based drug delivery systems reasonably, two model drugs were used as it has been proposed that drugs encapsulated in liposomes had influence on the ABC phenomenon. Doxorubicin (DOX), as a non-cell cycle specific drug, would abrogate the ABC phenomenon resulted from the reduced production of anti-PEG IgM by the inhibition of splenic B cells proliferation [15,16]. Topotecan hydrochloride (TPT), as a cell cycle specific drug, could only inhibit the population of splenic B cells occupying S phase, and its toxicity was dramatically limited [17]. Therefore, PCBylated and PEGylated liposomes with these two drugs were constructed in our following work for investigating their effects during blood circulation.

The sizes of DSPE-PCB and DSPE-PEG drug-loaded liposomes were about 100–150 nm (Fig. 1A), which were preferable for tumor accumulation *via* the EPR effect [18]. Moreover, the zeta potential analyses demonstrated that both drug-loaded liposomes exhibited

nearly neutral surface charges, which would minimize the undesirable nonspecific protein adsorption [19]. The structures of both empty and drug-loaded liposomes were further observed with Cryo-TEM. The empty and drug-loaded liposomes all had spherical shape with smaller diameters of approximately 70 nm due to the dehydration during the samples preparation process. The intraliposomal DOX and TPT were presented as crystalline self-assembled fiber-like structures as the Doxil® (Fig. 1B) [20]. The encapsulation efficiency of both liposomes was relatively high, around 90–95%, and they had comparable drug loading contents (Supporting Information, Table S1).

The stability of liposomes is an important criterion for *in vivo* biomedical application. By monitoring the changes of hydrodynamic diameters at time intervals in the presence of 10% FBS, the serum stability of drug-loaded liposomes was investigated. Both modified liposomes were stable over 96 h at 37 °C and there were only slight changes of the sizes (Supporting Information, Fig. S1A). Moreover, they exhibited superior physical stability at 4 °C for 27 d (Supporting Information, Fig. S1B). These results were in agreement with the previous study that the presence of PCB could avoid protein adsorption and enhance the stability of liposomes as that for PEG [21,22].

The drug release kinetics of the liposomes was detected at both the physiological pH of 7.4 and the endosomal pH of 5.0 by dialysis method, using DOX as a probe (Fig. 1C) [23–25]. Compared with free DOX, there was no significant initial burst release at pH 7.4 for

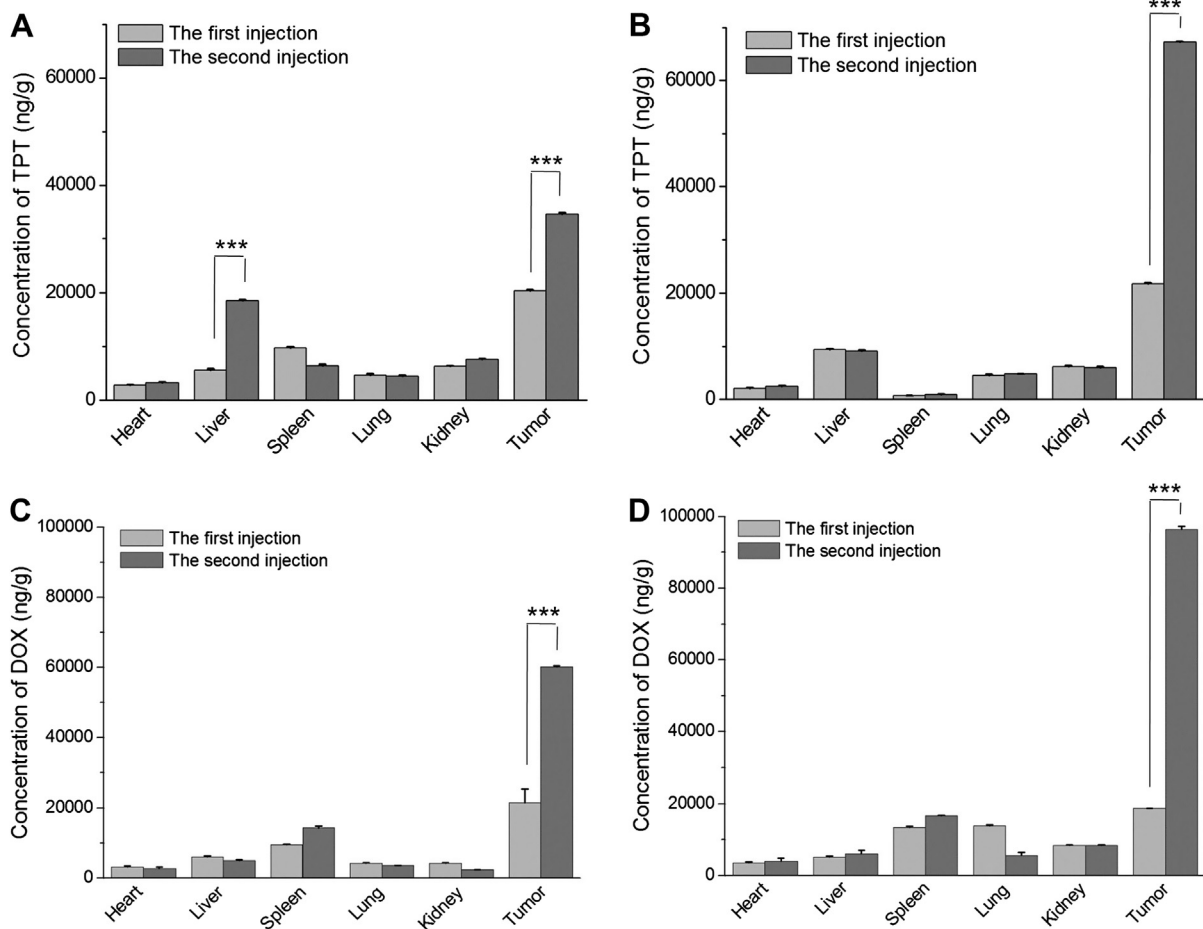


**Fig. 6.** *In vivo* distribution of drug-loaded liposomes on A549 tumor-bearing nude mice. A) DSPE-PEG TPT-liposomes. B) DSPE-PCB TPT-liposomes. C) DSPE-PEG DOX-liposomes. D) DSPE-PCB DOX liposomes as the first and second injection. Mice were treated with two doses of drug-loaded liposomes with 5 mg drug/kg *via* the tail vein. The interval between the two injections was 5 days. The concentration of drugs was detected by HPLC after 4 h of injection ( $n = 3$ ).

both liposomes, suggesting that these two liposomes were largely stable at physiological condition. Notably, the DOX releasing from the PEGylated liposomes was only 10% at pH 5.0 within 96 h incubation, whereas the amount reached to approximately 65% for PCBylated liposomes. The sustained release in acidic condition for PCB modified liposomes might attribute to the protonation of carboxyl acid groups of PCB in acidic condition, resulting in extensive disruption of the liposomes and encapsulated drug release. To confirm the hypothesis, zeta potential of liposomes was detected in PBs solution with pH range from 7.4 to 3.5, which

represented the physiological pH and endosomal/lysosomal pH [26]. As shown in Fig. 1D, the zeta potential of DSPE-PEG DOX-liposomes had no significant change over the studied pH range, whereas DSPE-PCB DOX-liposomes showed an increased pH-dependent zeta potential, from 2.51 mV at pH 7.4 to 15.3 mV at pH 3.5. The hypothesis was also approved by the changes of the diameters of liposomes at pH 7.4 and 5.0. As expectedly, the diameter of DSPE-PEG DOX-liposomes had no significant change at pH 7.4 and 5.0 till 36 h incubation. In contrast, DSPE-PCB DOX-liposomes were stable at pH 7.4 and the diameter was increased

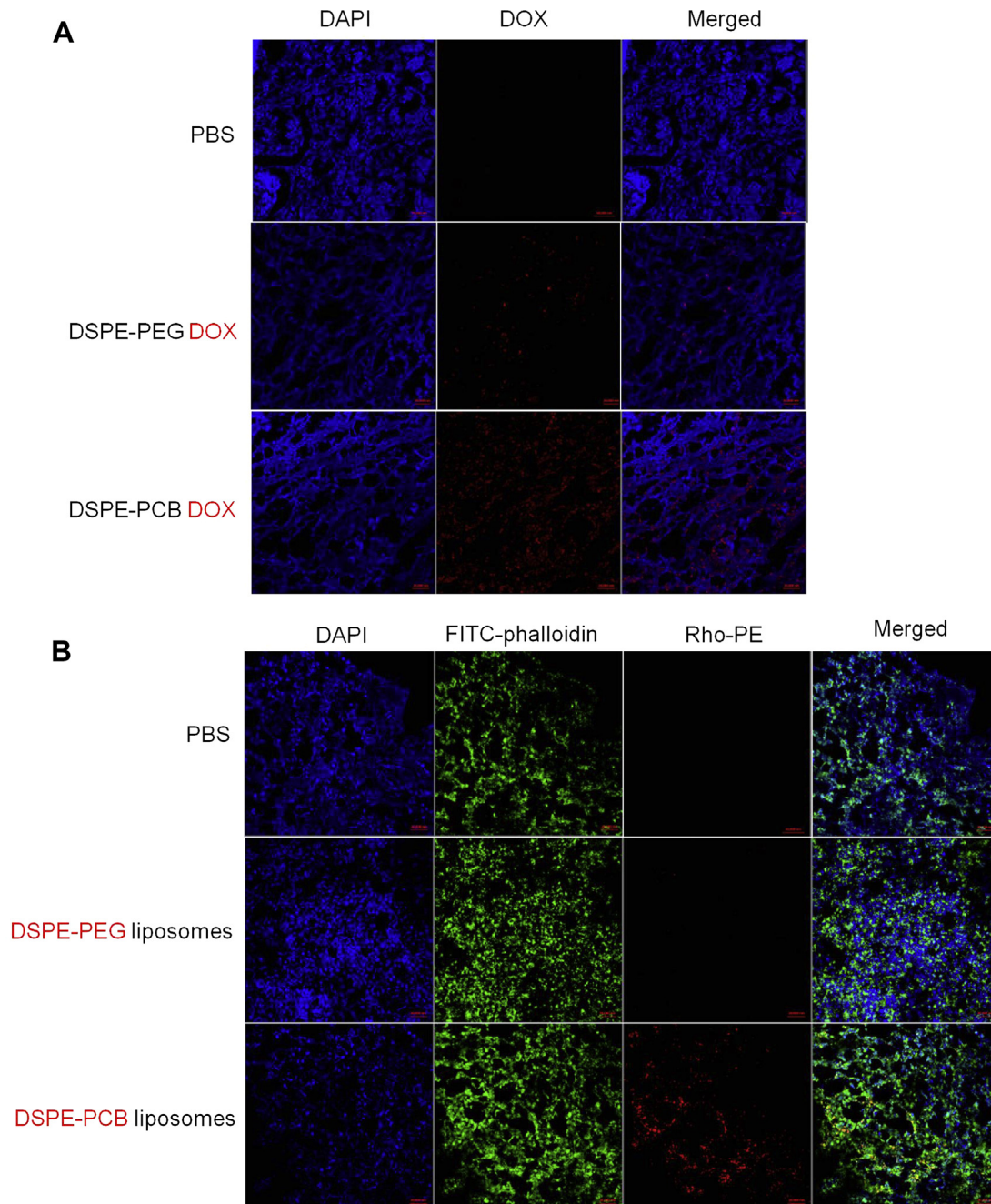


**Fig. 7.** The intra-tumor distribution of drug, PCB or PEG modified liposomes in tumor tissue observed using CLSM. (A) DOX fluorescent images of tumor tissue. (B) Rhodamine B labeled liposomes fluorescent images of tumor tissue. Mice were treated with DOX-loaded liposomes with 5 mg drug/kg or rhodamine B labeled empty liposomes with the same dose *via* the tail vein. The tumor tissues were obtained 24 h after injection. DAPI and FITC-phalloidin were used to stain the cell nucleus and microfilament skeleton in cytoplasm, respectively.

from 133.1 nm to 685.2 nm at pH 5.0 (Fig. 1E), which was also corroborated by Cryo-TEM (Fig. 1F). The results demonstrated that the protonation of PCB destabilized the liposomes by electrostatic repulsion at acidic environment, thereby promoting the drug release.

### 3.2. Cellular uptake behavior of drug-loaded liposomes

With different drug release ability of PCBylated and PEGylated liposomes, the intracellular trafficking of both drug-loaded liposomes was examined after incubation with A549 cells for 6 h, with

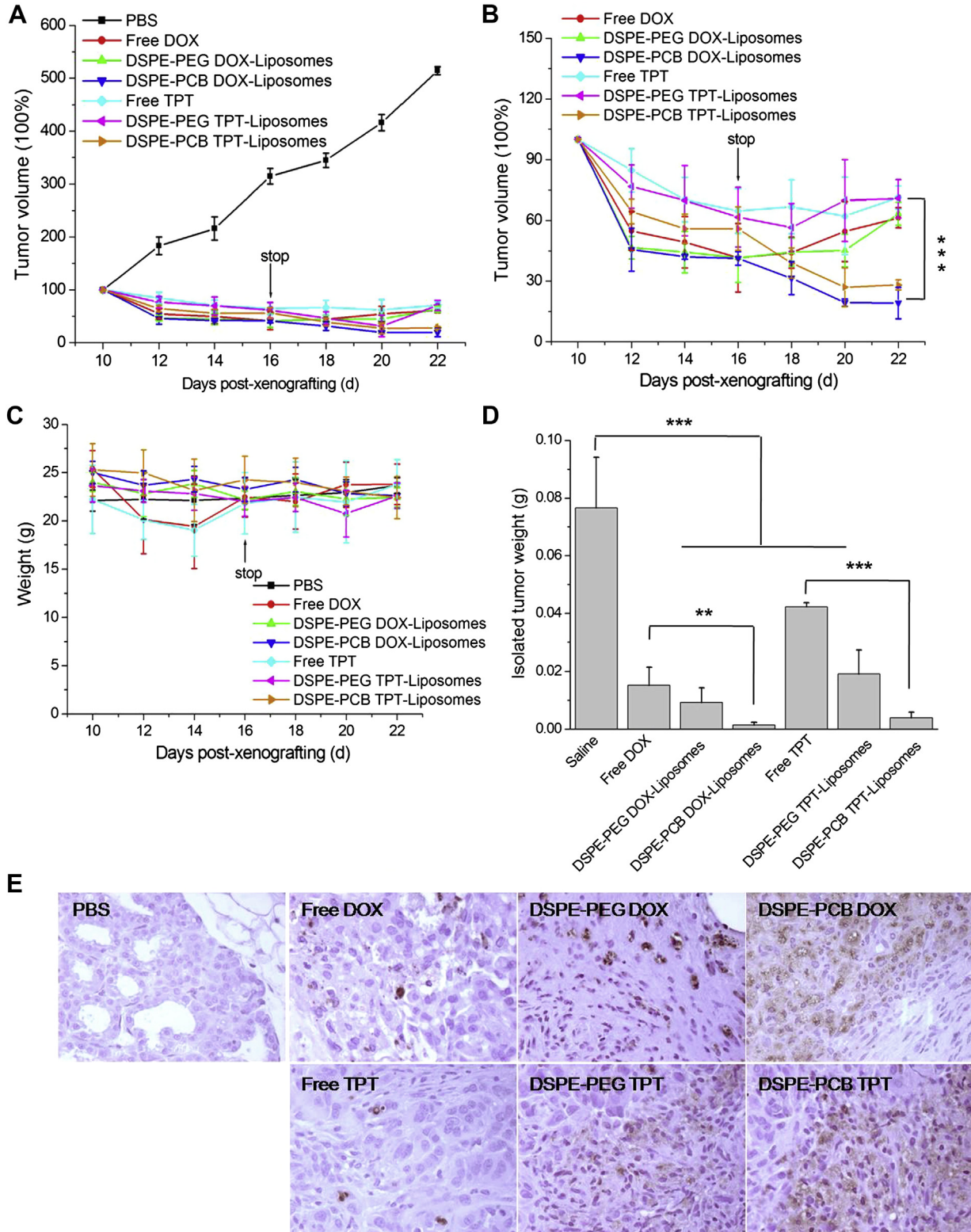


**Fig. 8.** The antitumor activity of free drugs and drug-loaded liposomes on A549 tumor-bearing nude mice. A) *In vivo* tumor growth inhibition. B) Tumor growth inhibition. C) Body weight changes. D) Tumor weight. E) TUNEL analyses of tumor tissue. Mice received one injection with 5 mg drug/kg *via* the tail vein every other day. The tumor tissues were collected after 12 days of treatment ( $n = 5$ ). \* $P < 0.05$ , \*\* $P < 0.01$ , \*\*\* $P < 0.005$ .

DOX as a fluorescence probe for flow cytometry analysis (Fig. 2A and Supporting Information, Fig. S2). The fluorescence intensity of DOX for DSPE-PCB liposomes was approximately 2 times of that for DSPE-PEG liposomes at the same time point, indicating that the DOX in PCBylated liposomes was more easily accumulated in cancer cells than that for PEGylated liposomes. It should also be noted that free DOX exhibited much stronger fluorescence intensity. It has been proved that free DOX was internalized into cells by direct diffusion, thus the free DOX accumulated in cells more quickly [27]. However, the cellular internalization mechanism of these drug-loaded liposomes has not been verified. The mechanism of the cellular internalization of DSPE-PEG and DSPE-PCB drug-loaded liposomes was further probed by performing the cellular uptake study at 4 °C or in the presence of various endocytic inhibitors. The cell internalization of both liposomes was mainly energy-dependent process, as about 65% of the cellular uptake was blocked at 4 °C (Fig. 2B). Genistein, chlorpromazine, dynasore and wortmannin all significantly inhibited the cellular uptake level of DSPE-PCB liposomes, indicating that PCBylated liposomes could also be internalized *via* endocytosis (Scheme 2) [28]. However, there was no significant change of cellular uptake for DSPE-PEG DOX-loaded liposomes, demonstrating that the encapsulated DOX might be internalized *via* diffusion after extracellular releasing from liposomes [29–31].

The data from spinning disk confocal image confirmed the different internalization process between DSPE-PEG and DSPE-PCB drug-loaded liposomes. The free DOX was internalized into cells by direct diffusion (Fig. 2C and Video 1). The rhodamine B labeled DSPE-PEG liposomes had no interaction with A549 cells due to the reduced interactions between PEGylated liposomes and the surface of the target cell, that the DOX was internalized *via* diffusion after extracellular releasing from liposomes (Fig. 2C and Videos 2,3) [32]. In contrast, DSPE-PCB liposomes were internalized *via* endocytosis with excellent cellular uptake (Fig. 2C and Videos 4,5). The difference in cellular internalization mechanism might be attributed to the different chemical structures of PCB and PEG, as PCB has positive charge groups, which might interact with negatively charged cell membrane and promote the cellular uptake of PCBylated liposomes *via* endocytosis. Furthermore, the intracellular distribution observed using CLSM indicated the excellent endosomal/lysosomal escape of DSPE-PCB drug-loaded liposomes after endocytosis (Supporting Information, Fig. S3). By changing the cellular uptake behavior, DSPE-PCB drug-loaded liposomes induced stronger cell cytotoxicity and apoptosis than that of DSPE-PEG drug-loaded liposomes *in vitro* (Supporting Information, Fig. S4). Additionally, both empty liposomes showed neglectable cytotoxicity at the studied concentration, indicating that PCBylated liposomes had excellent biocompatibility as that for PEGylated liposomes (Supporting Information, Fig. S5).

Supplementary video related to this article can be found at <http://dx.doi.org/10.1016/j.biomaterials.2014.11.010>.

### 3.3. Pharmacokinetics behavior of drug-loaded liposomes in SD rats

PEGylated liposomes with TPT could induce ABC phenomenon after repeated administration and its clinical use was significantly impeded. However, whether PCBylation liposomes would avoid ABC phenomenon *in vivo* has not been verified. To answer the question, three doses of liposomes were injected into rats with a time interval of 5 days. Pretreatment rats with DSPE-PEG TPT-liposomes triggered a rapid clearance of the second and third dose from the circulatory system (Fig. 3A). For DSPE-PCB TPT-liposomes, the blood clearance trend of TPT was basically the same for the three injections (Fig. 3B). The result indicated that PCBylated liposomes with cell cycle specific drugs could avoid the ABC

phenomenon. Furthermore, when rats were received repeated injections of DOX-loaded liposomes, the concentration of DOX in plasma was the same, suggesting no ABC phenomenon was elicited for DOX-loaded liposomes (Fig. 3C and D). To eliminate the drug influence, empty liposomes were administrated as the first injection to evaluate the PCBylation's effect on the ABC phenomenon. The results showed that DSPE-PEG empty liposomes induced significant ABC phenomenon that severely accelerated the blood clearance rate of DSPE-PEG DOX-liposomes for the second injection, which was comparable with that of free drugs. However, the ABC phenomenon was attenuated for the third injection due to the cytotoxicity of DOX to the splenic B cells after the second injection (Fig. 3E and Supporting Information, Fig. S6). On the other hand, no significant difference was found in the DOX concentration in plasma for DSPE-PCB liposomes after the empty liposomes injection (Fig. 3F). It suggested that PEGylated liposomes could stimulate ABC phenomenon by themselves after repeated injections, although the phenomenon would be eliminated when DOX was encapsulated. The DSPE-PCB liposomes could abrogate ABC phenomenon neither drug encapsulated or nor.

### 3.4. IgM level in plasma

It has been confirmed that there was a positive correlation between the anti-PEG IgM production and the accelerated clearance of PEGylated liposomes [33]. Whether the PCBylated liposomes would initiate the production of anti-PCB IgM was tested by administration of DSPE-PCB liposomes on rats. The IgM level in plasma was detected using ELISA 5 days later. DSPE-PEG TPT-liposomes induced the production of IgM for 4 to 5 times as the PBS groups after the first and second injection (Fig. 4A), while the IgM level for both DOX-liposomes was similar (Fig. 4B). Additionally, the first injection of DSPE-PEG empty liposomes induced obvious IgM increment, and the increment was reduced by administrating DSPE-PEG DOX-liposomes as the second injection due to the cytotoxicity of DOX to splenic B cells (Fig. 4C). The results clarified that DSPE-PEG empty liposomes or with cell cycle specific drug could induce the production of anti-PEG IgM, although the phenomenon was eliminated by DOX. As expectedly, there was no difference in IgM level for DSPE-PCB liposomes whatever the drug encapsulation compared with PBS group (Fig. 4A–C), demonstrating that DSPE-PCB modification could avoid the production of anti-PCB IgM, resulting in no ABC phenomenon.

To determine whether the generated IgM specifically bound to DSPE-PEG liposomes, the PEGylated and PCBylated liposomes were incubated with plasma obtained from rats received DSPE-PEG TPT, DOX and empty liposomes, respectively. As shown in Fig. 4D, the IgM level of DSPE-PEG liposomes groups in supernatant was severely decreased after incubation with the plasma received from DSPE-PEG TPT and empty liposomes groups. By contrast, there was no change of IgM level after incubation with DSPE-PCB liposomes for the same groups. It supported the idea that the elevated IgM selectively bound to DSPE-PEG liposomes.

### 3.5. Pharmacokinetics and biodistribution of drug-loaded liposomes in tumor-bearing mice

To further improve the conclusion, the pharmacokinetics behavior of both drug-loaded liposomes in A549 tumor-bearing nude mice was investigated. As shown in Fig. 5A and C, the results were in line with the pharmacokinetic results in rats that DSPE-PEG TPT-liposomes induced ABC phenomenon and accelerated the blood clearance for the second injection. While there was no significantly difference in pharmacokinetic profile for DSPE-PCB drug-loaded liposomes between the two doses (Fig. 5B and

D), indicated that DSPE-PCB liposomes could avoid ABC phenomenon.

The ABC phenomenon against the following dose of DSPE-PEG liposomes might interfere with its accumulation in tumor site. To demonstrate this, the biodistribution was analyzed after two injections with a time interval of 5 days on A549 tumor-bearing nude mice. In comparison with free drugs, all liposomal formulations significantly enhanced the drug accumulation in tumor due to the EPR effect (Supporting Information, Fig. S7) [34,35]. When mice were received DSPE-PEG TPT-liposomes, the TPT concentration in liver of the second dose was 3 times of that for the first injection (Fig. 6A), while the TPT accumulation in tumor of the second dose was only 0.59 times of that for DSPE-PCB TPT-liposomes (Fig. 6B). This indicated that the ABC phenomenon induced by DSPE-PEG TPT-liposomes increased drug accumulation in liver and decreased its accumulation in tumor. As expected, the concentration of DOX in liver for the second injection was equal to that for the first injection for DSPE-PEG DOX-liposomes (Fig. 6C), but the concentration of DOX in tumor for the second injection was still lower than that of DSPE-PCB liposomes (Fig. 6D). Compared with DSPE-PEG DOX-liposomes, the higher accumulation of DOX in tumor for DSPE-PCB liposomes was due to their readily cellular uptake into tumor cells *via* endocytosis.

The intra-tumor distribution of DOX and liposomes were further observed using CLSM. As shown in Fig. 7A, the fluorescence intensity of DOX for DSPE-PCB liposomes was much higher than that of DSPE-PEG liposomes and the DOX was mainly colocalized with the nucleus. The fluorescence intensity of rhodamine B labeled DSPE-PCB liposomes were colocalized with the fluorescence of FITC-phalloidin, which labeled the microfilament skeleton in cytoplasm, while there was no significant rhodamine B labeled DSPE-PEG liposomes signal (Fig. 7B). The results confirmed that PCBylated liposomes were taken up more efficiently by tumor cells, which resulted in higher efficacy drug molecules delivery.

### 3.6. Antitumor efficacy of drug-loaded liposomes *in vivo*

To provide *in vivo* evidence for the antitumor potential of the DSPE-PCB drug-loaded liposomes, the antitumor efficacy was investigated on A549 tumor-bearing nude mice. Compared with the control group, the tumor growth was effectively inhibited in all the drug groups (Fig. 8A and B). Free drugs delayed the tumor growth with the final relative tumor volume (RTV) of about 62%, but the body weight decreased obviously (Fig. 8C), which indicated the severe toxicity. DSPE-PCB liposomes had excellent antitumor activity, with 19.2% and 28.1% in the case of DOX and TPT, which was much better than that of DSPE-PEG liposomes (63.4% for DOX-liposomes and 70.8% for TPT-liposomes) due to their excellent tumor accumulation and cellular internalization. The drug-loaded liposomes exhibited neglectable toxicity, which indicated the good biocompatibility of PCBylated and PEGylated liposomes. The excised tumors exhibited the corresponding weight (Fig. 8D). Cell apoptosis in tumors and normal organs treated with various formulations was analyzed by the terminal deoxynucleotidyl transferase-mediated dUPT nick end-labeling (TUNEL) and hematoxylin-eosin staining (HE) (Fig. 8E and Supporting Information, Fig. S8). The DSPE-PCB drug-loaded liposomes induced much more significant cell apoptosis in tumors compared with free drugs and DSPE-PEG drug-loaded liposomes without obvious toxicity to other organs.

## 4. Conclusion

In summary, we successfully developed zwitterionic PCB modified liposome-based drug delivery systems. Quite different

from the DSPE-PEG liposomes, the pH-sensitive PCBylated liposomes changed the cellular uptake behavior of drug-loaded liposomes and were internalized into cells *via* endocytosis with excellent cellular uptake and drug release ability. Furthermore, the DSPE-PCB modified liposomes would avoid ABC phenomenon, which promoted the tumor accumulation of drug-loaded liposomes. With higher tumor accumulation and cellular uptake, the DSPE-PCB liposome-based drug delivery systems significantly inhibited tumor growth and provided a promising approach for cancer therapy.

## Acknowledgments

This work was financially supported by the National Natural Science Foundation of China (21304099, 51203162, 51103159, 51373177), the National High Technology Research and Development Program (2014AA020708, 2012AA022703, 2012AA020804), the Instrument Developing Project of the Chinese Academy of Sciences (YZ201253, YZ201313), the Open Funding Project of the National Key Laboratory of Biochemical Engineering (YZ2504A169) and the “Strategic Priority Research Program” of the Chinese Academy of Sciences (XDA09030301-3).

## Appendix A. Supplementary data

Supplementary data related to this article can be found at <http://dx.doi.org/10.1016/j.biomaterials.2014.11.010>.

## References

- [1] Maksimenko A, Dosio F, Mougny J, Ferrero A, Wack S, Reddy LH, et al. A unique squalenoylated and nonpegylated doxorubicin nanomedicine with systemic long-circulating properties and anticancer activity. *Proc Natl Acad Sci U S A* 2014;111:217–26.
- [2] Lee SM, Park HK, Yoo H. Synergistic cancer therapeutic effects of locally delivered drug and heat using multifunctional nanoparticles. *Adv Mater* 2010;22:4049–53.
- [3] Chiang YT, Lo CL. pH-Responsive polymer-liposomes for intracellular drug delivery and tumor extracellular matrix switched-on targeted cancer therapy. *Biomaterials* 2014;35:5414–24.
- [4] Li CL, Cao JN, Wang YJ, Zhao X, Deng CX, Wei N, et al. Accelerated blood clearance of PEGylated liposomal topotecan: influence of polyethylene glycol grafting density and animal species. *J Pharm Sci* 2012;101:3864–76.
- [5] Yuan YY, Mao CQ, Du XJ, Du JZ, Wang F, Wang J. Surface charge switchable nanoparticles based on zwitterionic polymer for enhanced drug delivery to tumor. *Adv Mater* 2012;24:5476–80.
- [6] Hong BJ, Chipre AJ, Nguyen ST. Acid-degradable polymer-caged lipoplex (PCL) platform for siRNA delivery: facile cellular triggered release of siRNA. *J Am Chem Soc* 2013;135:17655–8.
- [7] Ishida T, Harada M, Wang XY, Ichihara M, Irimura K, Kiwada H. Accelerated blood clearance of PEGylated liposomes following preceding liposome injection: effects of lipid dose and PEG surface-density and chain length of the first-dose liposomes. *J Control Release* 2005;105:305–17.
- [8] Judge A, McClintock K, Phelps JR, MacLachlan I. Hypersensitivity and loss of disease site targeting caused by antibody responses to PEGylated liposomes. *Mol Ther* 2006;13:328–37.
- [9] Li A, Luehmann HP, Sun GR, Samarajeewa S, Zou J, Zhang SY, et al. Synthesis and *in vivo* pharmacokinetic evaluation of degradable shell cross-linked polymer nanoparticles with poly(carboxybetaine) versus poly(ethylene glycol) surface-grafted coatings. *ACS Nano* 2012;6:8970–82.
- [10] Ishida T, Ichihara M, Wang XY, Kiwada H. Spleen plays an important role in the induction of accelerated blood clearance of PEGylated liposomes. *J Control Release* 2006;115:243–50.
- [11] Abu LAS, Nawata K, Shimizu T, Ishida T, Kiwada H. Use of polyglycerol (PG), instead of polyethylene glycol (PEG), prevents induction of the accelerated blood clearance phenomenon against long-circulating liposomes upon repeated administration. *Int J Pharm* 2013;456:235–42.
- [12] Xu H, Wang QQ, Deng YH, Chen DW. Effects of cleavable PEG-cholesterol derivative on the accelerated blood clearance of PEGylated liposomes. *Biomaterials* 2010;31:4757–63.
- [13] Ishihara T, Maeda T, Sakamoto H, Takasaki N, Shigyo M, Ishida T, et al. Evasion of the accelerated blood clearance phenomenon by coating of nanoparticles with various hydrophilic polymers. *Biomacromolecules* 2010;11:2700–6.

- [14] Li Y, Cheng Q, Jiang Q, Huang YY, Liu HM, Zhao YL, et al. Enhanced endosomal/lysosomal escape by distearoyl phosphoethanolamine-polycarboxybetaine lipid for systemic delivery of siRNA. *J Control Release* 2014;176:104–14.
- [15] Ishida T, Atobe K, Wang XY, Kiwada H. Accelerated blood clearance of PEGylated liposomes upon repeated injections: effect of doxorubicin-encapsulation and high-dose first injection. *J Control Release* 2006;115:251–8.
- [16] Abu Lila AS, Kiwada H, Ishida T. The accelerated blood clearance (ABC) phenomenon: clinical challenge and approaches to manage. *J Control Release* 2013;172:38–47.
- [17] Li CL, Zhao X, Wang YJ, Yang HY, Li HX, Li H, et al. Prolongation of time interval between doses could eliminate accelerated blood clearance phenomenon induced by PEGylated liposomal topotecan. *Int J Pharm* 2013;443:17–25.
- [18] Liao LY, Liu J, Dreaden EC, Morton SW, Shopsowitz KE, Hammond PT, et al. A convergent synthetic platform for single-nanoparticle combination cancer therapy: ratiometric loading and controlled release of cisplatin, doxorubicin, and camptothecin. *J Am Chem Soc* 2014;136:5896–9.
- [19] Xiao K, Li YP, Luo JT, Lee JS, Xiao WW, Gonik AM, et al. The effect of surface charge on *in vivo* biodistribution of PEG-oligocholic acid based micellar nanoparticles. *Biomaterials* 2011;32:3435–46.
- [20] Barenholz Y. Doxil<sup>®</sup> – the first FDA-approved nano-drug: lessons learned. *J Control Release* 2012;160:117–34.
- [21] Zhang L, Xue H, Cao ZQ, Keefe A, Wang JN, Jiang SY. Multifunctional and degradable zwitterionic nanogels for targeted delivery, enhanced MR imaging, reduction-sensitive drug release, and renal clearance. *Biomaterials* 2011;32:4604–8.
- [22] Dai FY, Liu WG. Enhanced gene transfection and serum stability of polyplexes by PDMAEMA-polysulfobetaine diblock copolymers. *Biomaterials* 2011;32:628–38.
- [23] Liang K, Richardson JJ, Ejima H, Such GK, Cui JW, Caruso F. Peptide-tunable drug cytotoxicity *via* one-step assembled polymer nanoparticles. *Adv Mater* 2014;26:2398–402.
- [24] Mo R, Sun Q, Xue JW, Li N, Li WY, Zhang C, et al. Multistage pH-responsive liposomes for mitochondrial-targeted anticancer drug delivery. *Adv Mater* 2012;24:3659–65.
- [25] Wang JQ, Sun XR, Mao WW, Sun WL, Tang JB, Sui MH, et al. Tumor redox heterogeneity-responsive prodrug nanocapsules for cancer chemotherapy. *Adv Mater* 2013;25:3670–6.
- [26] Duan XP, Xiao JS, Yin Q, Zhang ZW, Yu HJ, Mao SR, et al. Smart pH-sensitive and temporal-controlled polymeric micelles for effective combination therapy of doxorubicin and disulfiram. *ACS Nano* 2013;7:5858–69.
- [27] Kim J, Jee JE, Lee SH, Yu JH, Lee JH, Park TG, et al. Designed fabrication of a multifunctional polymer nanomedical platform for simultaneous cancer-targeted imaging and magnetically guided drug delivery. *Adv Mater* 2008;20:478–83.
- [28] Yin LC, Song ZY, Kim KH, Zheng N, Tang HY, Lu H, et al. Reconfiguring the architectures of cationic helical polypeptides to control non-viral gene delivery. *Biomaterials* 2013;34:2340–9.
- [29] Chen KJ, Chaung EY, Wey SP, Lin KJ, Cheng F, Lin CC, et al. Hyperthermia-mediated local drug delivery by a bubble-generating liposomal system for tumor-specific chemotherapy. *ACS Nano* 2014;8:5105–15.
- [30] Allen TM, Cullis PR. Drug delivery systems: entering the mainstream. *Science* 2004;303:1818–22.
- [31] Kong G, Anyarambhatla G, Petros WP, Braun RD, Colvin OM, Needham D, et al. Efficacy of liposomes and hyperthermia in a human tumor xenograft model: importance of triggered drug release. *Cancer Res* 2000;15:6950–7.
- [32] Qhatal HSS, Hye T, Alali A, Liu XL. Hyaluronan polymer length, grafting density, and surface poly(ethylene glycol) coating influence *in vivo* circulation and tumor targeting of hyaluronan-grafted liposomes. *ACS Nano* 2014;8:5423–40.
- [33] Hashimoto Y, Abu Lila AS, Shimizu T, Ishida T, Kiwada H. B cell-intrinsic toll-like receptor 7 is responsible for the enhanced anti-PEG IgM production following injection of siRNA-containing PEGylated lipoplexes in mice. *J Control Release* 2014;184:1–8.
- [34] Fang J, Nakamura H, Maeda H. The EPR effect: unique features of tumor blood vessels for drug delivery, factors involved, and limitations and augmentation of the Effect. *Adv Drug Deliv Rev* 2011;63:136–51.
- [35] Torchilin V. Tumor delivery of macromolecular drugs based on the EPR effect. *Adv Drug Deliv Rev* 2011;63:131–5.